

Elsevier Editorial System(tm) for Applied
Surface Science
Manuscript Draft

Manuscript Number: APSUSC-D-16-11991R1

Title: Shape-dependent antibacterial activity of silver nanoparticles on
Escherichia.coli and Enterococcus.faecium bacterium

Article Type: SI: ICPAM-11

Keywords: Keywords: AgNPs, shape-dependent, antibacterial activity,
E.coli and Enterococcus sp

Corresponding Author: Mrs. Alanod Alshareef, PHD

Corresponding Author's Institution: De Montfort university

First Author: Alanod Alshareef, PHD

Order of Authors: Alanod Alshareef, PHD; Katie laird, Head of the
Infectious Disease Research Group; Richard Cross, Research Fellow

Shape-dependent antibacterial activity of silver nanoparticles on *Escherichia.coli* and *Enterococcus.faecium* bacterium

A, Alshareef¹, K, Laird² and R. B. M. Cross¹

¹Emerging Technologies Research Centre, School of Engineering and Sustainable Development, Faculty of Technology, De Montfort University, Leicester, LE19BH, United Kingdom; ²Leicester School of Pharmacy, Infectious Disease Research Group, Faculty of Health and Life Sciences, De Montfort University, Leicester, LE19BH, United Kingdom

Corresponding author: R. B. M. Cross, rcross@dmu.ac.uk, +00441162506157

Abstract: Silver nanoparticles (AgNPs) have been shown to exhibit strong antibacterial activity against both Gram-positive bacteria and Gram-negative bacteria including antibiotic resistant strains. The antibacterial activity of AgNPs against *Escherichia coli* and *Streptococcus mutans* (*S. Mutans*) has been reported and found to be size dependent. This study aims to compare the bactericidal effect of different shaped AgNPs (spherical and truncated octahedral) against *E.coli* and *E.faecium*. The antimicrobial activity of a range of concentrations (50, 100, 1000µg/ml) was determined over 24 hours using both optical density and viable counts. Truncated octahedral AgNPs (AgNoct) were found to be more active when compared with spherical AgNPs (AgNS). The difference in shape resulted in differences in efficacy which may be due to the higher surface area of AgNOct compared to AgNS, and differences in active facets and surface energies, with AgNPs having a bacteriostatic effect and AgNOct is being bactericidal after 4 hours. The results suggest that AgNPs can be used as effective growth inhibitors in different microorganisms, rendering them applicable to various medical devices and antimicrobial control systems.

Highlights:

- Truncated octahedral AgNPs (AgNOct) were found to be more active when compared with spherical AgNPs (AgNS)
- AgNPs having a bacteriostatic effect and AgNOct is being bactericidal after 4 hours
- the bactericidal effect of AgNOct may be due to their geometric structure, higher surface area and higher surface energies
- The positively charged AgNPs are attracted electrostatically to the negatively charged lipopolysaccharides, teichoic acids in Gram negative and Gram-positive bacteria respectively which may then be ruptured followed by protein denaturation and cell death

Shape-dependent antibacterial activity of silver nanoparticles on *Escherichia coli* and *Enterococcus faecium* bacterium

A, Alshareef¹, K, Laird² and R. B. M. Cross¹

¹Emerging Technologies Research Centre, School of Engineering and Sustainable Development, Faculty of Technology, De Montfort University, Leicester, LE19BH, United Kingdom; ²Leicester School of Pharmacy, Infectious Disease Research Group, Faculty of Health and Life Sciences, De Montfort University, Leicester, LE19BH, United Kingdom

Corresponding author: R. B. M. Cross, rcross@dmu.ac.uk, +00441162506157

Abstract: Silver nanoparticles (AgNPs) have been shown to exhibit strong antibacterial activity against both Gram-positive bacteria and Gram-negative bacteria including antibiotic resistant strains. This study aims to compare the bactericidal effect of different shaped AgNPs (spherical and truncated octahedral) against *Escherichia coli* and *Enterococcus faecium*. The antimicrobial activity of a range of concentrations (50, 100, 1000µg/ml) was determined over 24 hours using both optical density and viable counts. Truncated octahedral AgNPs (AgNOct) were found to be more active when compared with spherical AgNPs (AgNS). The difference in shape resulted in differences in efficacy which may be due to the higher surface area of AgNOct compared to AgNS, and differences in active facets and surface energies, with AgNPs having a bacteriostatic effect and AgNOct being bactericidal after 4 hours. The results suggest that AgNPs can be used as effective growth inhibitors in different microorganisms, rendering them applicable to various medical devices and antimicrobial control systems.

Keywords: AgNPs, shape-dependent, antibacterial activity, *Escherichia coli* and *Enterococcus faecium*

1-Introduction

Increasing numbers of microbial organisms are becoming resistant to antibiotics demonstrating a need for new, effective antibacterial agents [1]. In this regard, nanoscale materials have emerged as potential candidates in this area due to their unique physical and chemical properties [2]. The antibacterial effects of silver (Ag) salt are well known, and have been utilised to control bacterial growth in various devices and applications; these include catheters, dentistry, burn wounds, coated medical devices and water filtration [3] [4]. Moreover, a potential benefit of the use of nanoscale Ag particles (AgNPs) against microorganisms, e.g. *Escherichia coli* and *Enterococcus faecium* [5], is that such organisms are unlikely to build up resistance against AgNPs due to their broad spectrum of activity, unlike the narrow-targets of conventional antibiotics [6]. This activity includes the ability to attach through electrostatic interaction to the cell membrane and penetrate inside the bacteria, where they interact with sulphur-containing proteins and phosphorus containing compounds such as DNA [7]. Also, they have been shown to act upon the respiratory chain and replication of the bacterial cells leading to cell death [8].

The antibacterial activity of AgNPs against *E.coli* and *Streptococcus mutans* has been investigated previously and found to be size dependent, demonstrating that AgNPs of 5nm exhibit higher antibacterial activity when compared to 15nm and 55nm particles in Gram-positive and Gram-negative bacteria [9]. The antimicrobial efficacy of NPs can also depend on their shape. *Pal et al.* (2007) showed truncated triangular AgNPs exhibit *E.coli* inhibition at 1 µg; however, in order for spherical NPs to inhibit *E.coli* 12.5 µg was required, with rod NPs needing a total of 50 to 100 µg of silver content [7]. In our previous work, copper nanocubes showed enhanced antibacterial activity on *E.coli* and *E.faecium* compared with copper nanospheres [10]. This study aims to determine shape dependence (spherical and truncated octahedral) on the antimicrobial efficacy of AgNP against *E.coli* and *E.faecium*.

2-Experiment

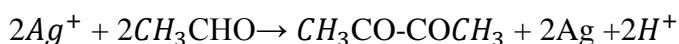
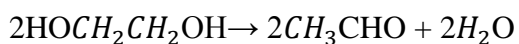
2.1-Materials

All chemicals for this work were purchased from Sigma-Aldrich, UK, without further purification. They include silver nitrate (AgNO_3), sodium bromide (NaBr),

polyvinylpyrrolidone (PVP) ($[C_6H_9NO]_n$), ethylene glycol (EG) ($C_2H_6O_2$) and sodium citrate ($C_6H_5Na_3$).

2.2-Synthesis of AgNOct

To synthesise AgNPOct, 3ml of two EG solutions, one containing 144mM PVP and 0.11mM NaBr, the other containing 94mM $AgNO_3$, were added dropwise via a two-channel syringe pump to 5ml of EG heated in a condenser at 160 °C. A 30 μ L drop of 10mM NaBr was then added to the pre-heated EG. The reaction solution turned yellow in a few seconds after the addition of $AgNO_3$ and PVP demonstrating the formation of AgNPs. After 10 minutes, the yellow colour faded in intensity due to oxidative etching and remained a light yellow colour for approximately 10 minutes before turning to brown and then to grey as the NPs increased in size. The synthesised NPs were then centrifuged at 4600rpm three times and washed with de-ionised water ((DI) 18.2M Ω MilliQ) to remove any impurities and unreacted precursors. The reactions governing the particles formation are expressed as follows [11]:

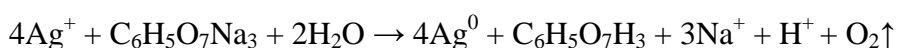


These reactions usually occur in the presence of a mediating species such as sodium bromide, sodium sulphide, sodium borohydride and hydrochloric acid. These mediators (NaBr in this case), play a role in the etching of the particle seeds, facilitating the formation of truncated octahedrons. The PVP also works as a shape-control agent prompting the reduction of $AgNO_3$ onto specific crystal faces while preventing reduction onto others.

2.3- Synthesis of AgNS

To synthesize spherical AgNPs, an aqueous solution of $AgNO_3$ 0.001M was heated to 100°C and then 3ml of sodium citrate was added. The mixture continued to be heated until the colour changed to yellow. To remove contamination and unreacted precursors from the AgNSs, a combination of centrifugation and DI water washes was used three times as before.

The particles were produced by reducing $AgNO_3$ through the following reaction [12]:



2.4-Particle characterisation

The AgNPs of both shapes were characterised using ultraviolet/visible (UV-VIS) spectroscopy (Evolution 300 UV-VIS, over the wavelength range 300nm to 700nm), scanning electron microscopy (SEM) and energy-dispersive X-ray (EDX) spectroscopy (LEO S430), and X-ray diffraction (XRD) Bruker D8 Advance diffractometer). The various solutions were drop-cast onto silicon and glass substrates for SEM/EDX and UV-VIS/XDR investigations respectively.

2.5-Antibacterial activity studies

All investigation were carried out in triplicate on at least two separate occasions

2.5.1-Bacterial strains and culture conditions

The antibacterial activities of the AgNPs were investigated using *E.coli* (NCTC8196) and *E.faecium* (NCTC12202) as models for Gram-negative bacteria and Gram-positive bacteria respectively. Bacteria strains were stored in Luria Bertani broth at -80°C; bacteria were then cultured in nutrient broth (NB) at 37 °C for 24 hours.

2.5.2- Screening of AgNPs for antibacterial activity

A disc diffusion method was used to determine the antibacterial activity of both shapes of AgNPs. In brief, overnight cultures of *E.coli* and *E. faecium* were spread-plated on to nutrient agar (NA), a 2cm paper disc was then impregnated with 50µl of 100µg/ml of both shapes of AgNPs and placed on the surface of the NA and incubated at 37°C for 24 hours. Zones of inhibition were then measured.

2.5.3-Determining the growth curve of *E. coli* and *E. faecium* bacteria cells exposed to different concentration of AgNPs using optical density

To investigate the growth kinetics curves of bacterial cells exposed to AgNPs different concentrations of both shapes (1000 µg, 100 µg and 50 µg) were used. Aliquots of 200µl of either *E.coli* or *E. faecium* in the presence of AgNPs were dispensed into 96-well plates. Optical densities (OD) were measured every hour (from 0 to 24 hour) at 600nm using a spectrophotometer (Spectra Max Plus 384). The control was wells containing bacteria only.

2.5.4-Viable count growth curves

An overnight culture of either *E. coli* or *E. faecium*, was inoculated into fresh NB (10^8) containing either AgNOct or AgNS of 1000 μ g/ml. The cultures were then incubated at 37 °C in a shaking incubator and samples taken at 0, 2, 4, 6 and 24 h. Aliquots of 100 μ l were spread-plated on to NA and incubated at 37 °C for 24h. Plates were then enumerated.

3-Results and discussion

The absorption spectrum of the AgNOct solution in Figure 1a shows an intense peak at 485nm with shoulders at 345nm and 365nm. The shape and position of plasmon absorption of AgNPs are mainly dependent on dielectric medium, particle size and the surface adsorbed species [5]. Anisotropic particles such as truncated octahedrons could have two or more SPR bands depending on the shape of the particles. However, only a single SPR band is present in the absorption spectra of spherical NPs. Figure 1b shows a sharp and intense peak at 410nm that is attributable to the surface plasmon absorption of spherical AgNPs [13].

SEM images of prepared AgNOct and AgNS are shown in Figure 2 (a and b respectively). The AgNOct have an average diameter of \sim 194nm. The size distribution is calculated from SEM images, where the polydispersity is 25% (Figure 3a). Figure 2b shows spherically-shaped NPs having an average diameter of \sim 195nm, where the polydispersity is 26% (Figure 3b). EDX analysis of the AgNPs shows the high purity of both sets of samples (Figure4 a and b).

XRD data shown in Figure 5 (a and b) confirms the formation of FCC AgNPs. Diffraction peaks at 2θ are 38, 44, 64, 77, 81, which are attributed to (111), (200), (202), (311) and (222) lattice planes of Ag with a cubic phase (JCPDS card no. 04-0783). AgNOct have higher intensities of (200), (202), (311) and (222) lattice planes compared with AgNS. Generally, spherical AgNPs exhibit a dominant (100) peak, while truncated octahedron AgNPs exhibit (111) with a lower intensity of (100). It has been reported previously that the reactivity of Ag is enhanced by high atomic density facets such as (111) [5][14]. It was postulated that atoms were more reactive on the facets of higher surface energy, which may

lead them to interact rapidly with oxygen-containing groups of lipopolysaccharide molecules that can result in enhanced attachment to the cell membrane [14].

Screening data shows that both shapes of AgNPs inhibit the growth of *E.coli* and *E. faecium* (the zone of inhibition was 2cm for both bacteria), as inhibition only occurred where there was direct contact with the AgNPs. The efficacy of spherical and truncated octahedral AgNPs was elucidated against *E.coli* and *E. faecium* using optical density. *E.coli* treated with AgNOct showed completely inhibited growth for all concentrations (1000, 100, 50 μ g) (Figure 6). However, there was limited growth in *E. faecium* at lower concentrations (50, 100 μ g), with only 1000 μ g completely inhibiting (Figure 7). Consequently the inhibitory effects were higher in *E.coli* compared with *E. faecium* for AgNOct.

Inhibition of *E.coli* treated with AgNS occurred at 10 hours with 1000 μ g/ml (Figure 8). For *E. faecium*, inhibition occurred in the first 6 hours at the same concentration and then limited growth began to occur (Figure 9). When viable count growth curves were generated in the presence of 1000 μ g/ml for both AgNOct and AgNS, the use of AgNOct against both bacteria resulted in the organisms being killed after 4 hours, demonstrating a bactericidal effect. Whereas, in the presence of AgNS there was only a modest reduction in CFU/mls in both organisms, demonstrating a bacteriostatic effect (Figure 10 and Figure 11). The viable count growth curves for untreated *E.coli* and *E. faecium* are shown in Figure 12 as a control.

The surface area of AgNOct was 1.32 m^2/g , while for AgNS it was 1.26 m^2/g . The data in Table 1 suggests that the shape effect on the antibacterial activity of AgNPs may be attributed to the higher surface areas and facet reactivity; AgNPs with larger effective contact areas and higher reactive facets exhibit stronger antibacterial activity [15]. Moreover, the antibacterial activity of AgNOct may be related to their geometric structure where AgNOct exhibit higher intensities than AgNSs of (200), (202), (311) and (222) lattice planes that might result in an increase in antibacterial activity.

The greater inhibitory effects observed in *E.coli* than in *E. faecium* are attributed to differences in the structure and thickness of the peptidoglycan layer of their cell walls. The peptidoglycan layer of Gram-positive bacteria such as *E. faecium* (~20-80nm) is thicker than that in Gram-negative bacteria such as *E. coli* (~7-8nm), as it includes linear polysaccharide chains cross-linked by short peptides to make a three dimensional rigid structure. This makes it more difficult for NPs to attach and penetrate [16]. In addition, the positively charged AgNPs are attracted electrostatically to the negatively charged

lipopolysaccharides and teichoic acids in Gram negative and Gram-positive bacteria respectively; this may lead to rupture and protein denaturation followed by cell death [17].

4-Conclusion

During this study AgNOct and AgNS were synthesised by a chemical reduction method in EG and DI water respectively. The NPs were characterised using UV-VIS, SEM, EDX and XRD. The antimicrobial efficacy of the AgNPs has been shown to be shape dependent against the organisms tested. AgNOct demonstrate bactericidal activity compared with bacteriostatic behaviour of AgNS. It is suggested that the bactericidal effect of AgNOct may be due to their geometric structure, higher surface area and higher surface energies when compared to AgNSs. This higher reactivity may ultimately lead to cell death more rapidly. Work is ongoing to determine more fully the mechanisms of action of the AgNPs that lead to the demonstrated bactericidal effects.

References

- [1] J. S. Kim, E. Kuk, K. N. Yu, J. Kim, S. J. Park, H. J. Lee, S. H. Kim, Y. K. Park, Y. H. Park and C. Hwang, "Antimicrobial effects of silver nanoparticles," *Nanomedicine: Nanotechnology, biology and medicine*, vol 3, no 1, pp. 95-101, 2007.
- [2] M. Rai, A. Yadav and A. Gade, "Silver nanoparticles as a new generation of antimicrobials," *Biotechnology advances*, vol 27, no 1, pp. 76-83, 2009.
- [3] M. Catauro, M. Raucci, F. De Gaetano and A. Marotta, "Antibacterial and bioactive silver-containing $\text{Na}_2\text{O} \cdot \text{CaO} \cdot 2\text{SiO}_2$ glass prepared by sol-gel method," *Journal of materials science: Materials in medicine*, vol 15, no 7, pp. 831-837, 2004.
- [4] J. H. Crabtree, R. J. Burchette, R. A. Siddiqi, I. T. Huen, L. L. Hadnott and A. Fishman, "The efficacy of silver-ion implanted catheters in reducing peritoneal dialysis-related infections," *Peritoneal dialysis international : Journal of the international society for peritoneal dialysis*, vol 23, no 4, pp. 368-374, Jul-Aug 2003.
- [5] S. Pal, Y. K. Tak and J. M. Song, "Does the antibacterial activity of silver nanoparticles depend on the shape of the nanoparticle? A study of the gram-negative bacterium escherichia coli," *Applied and environmental microbiology*, vol 73, no 6, pp. 1712-1720, Mar 2007.

- [6] G. Zhao and S. E. Stevens, "Multiple parameters for the comprehensive evaluation of the susceptibility of escherichia coli to the silver ion," *Biometals*, vol 11, no 1, pp. 27-32, 1998.
- [7] B. Sadeghi, F. S. Garmaroudi, M. Hashemi, H. Nezhad, A. Nasrollahi, S. Ardalan and S. Ardalan, "Comparison of the anti-bacterial activity on the nanosilver shapes: Nanoparticles, nanorods and nanoplates," *Advanced powder technology*, vol 23, no 1, pp. 22-26, 2012.
- [8] I. Sondi and B. Salopek-Sondi, "Silver nanoparticles as antimicrobial agent: A case study on E. coli as a model for gram-negative bacteria," *Journal of colloid and interface science*, vol 275, no 1, pp. 177-182, 2004.
- [9] Z. Lu, K. Rong, J. Li, H. Yang and R. Chen, "Size-dependent antibacterial activities of silver nanoparticles against oral anaerobic pathogenic bacteria," *Journal of materials science: Materials in medicine*, vol 24, no 6, pp. 1465-1471, 2013.
- [10] A. Alshareef, K. Laird and R. Cross, "Chemical synthesis of copper nanospheres and nanocubes and their antibacterial activity against escherichia coli and enterococcus sp." *Acta metallurgica sinica (english letters)*, pp. 1-7, 2016.
- [11] B. Gupta, W. Rouesnel and J. J. Gooding, "The role of oxygen in synthesizing monodisperse silver nanocubes," *Australian journal of chemistry*, vol 64, no 11, pp. 1488-1493, 2011.
- [12] C. RATYAKSHI. R.P, " Colloidal synthesis of silver nano particles " *Asian journal of chemistry*, vol Vol. 21, no No. 10, pp. S113-116, 2009.
- [13] M. Guzman, J. Dille and S. Godet, "Synthesis and antibacterial activity of silver nanoparticles against gram-positive and gram-negative bacteria," *Nanomedicine: Nanotechnology, biology and medicine*, vol 8, no 1, pp. 37-45, 2012.
- [14] Y. Xia, Y. Xiong, B. Lim and S. E. Skrabalak, "Shape Controlled synthesis of metal nanocrystals: Simple chemistry meets complex physics?" *Angewandte chemie international edition*, vol 48, no 1, pp. 60-103, 2009.
- [15] X. Hong, J. Wen, X. Xiong and Y. Hu, "Shape effect on the antibacterial activity of silver nanoparticles synthesized via a microwave-assisted method," *Environmental science and pollution research*, vol 23, no 5, pp. 4489-4497, 2016.
- [16] W. Wang, L. Geng, S. Ding and S. Xu, , "Facile synthesis of silver nanoparticles and their antimicrobial activity against several representative microbial species," In *Biomedical engineering and biotechnology (iCBEB), 2012 international conference on*, 2012, pp. 287-290.
- [17] A. M. Fayaz, K. Balaji, M. Girilal, R. Yadav, P. T. Kalaichelvan and R. Venketesan, "Biogenic synthesis of silver nanoparticles and their synergistic effect with antibiotics: A study against gram-positive and gram-negative bacteria," *Nanomedicine: Nanotechnology, biology and medicine*, vol 6, no 1, pp. 103-109, 2010.

List of Figures:

Figure 1: UV absorption spectra (a) AgNOct, (b) AgNS.

Figure 2: SEM images of (a) AgNOct, (b) AgNS.

Figure 3: Size distribution for (a) AgNOct, (b) AgNS.

Figure 4: EDX of (a), AgNOct, (b) AgNS.

Figure 5: XRD pattern obtained from (a) AgNOct, (b) AgNS.

Figure 6: Growth curves (optical density) of *E.coli* treated with different concentration ($\mu\text{g/ml}$) of AgNOct

Figure 7: Growth curves (optical density) of *E.faecium* treated with different concentration ($\mu\text{g/ml}$) of AgNOct.

Figure 8: Growth curves (optical density) of *E.coli* treated with different concentration ($\mu\text{g/ml}$) of AgNS.

Figure 9: Growth curves (optical density) of *E.faecium* treated with different concentration ($\mu\text{g/ml}$) of AgNS.

Figure 10: Viable count growth curves in the presence of AgNOct and AgNS for *E.faecium*.

Figure 11: Viable count growth curves in the presence of AgNS and AgNOct for *E.coli*

Figure 12: Viable count growth curves of untreated *E.coli* and *E. faecium*.

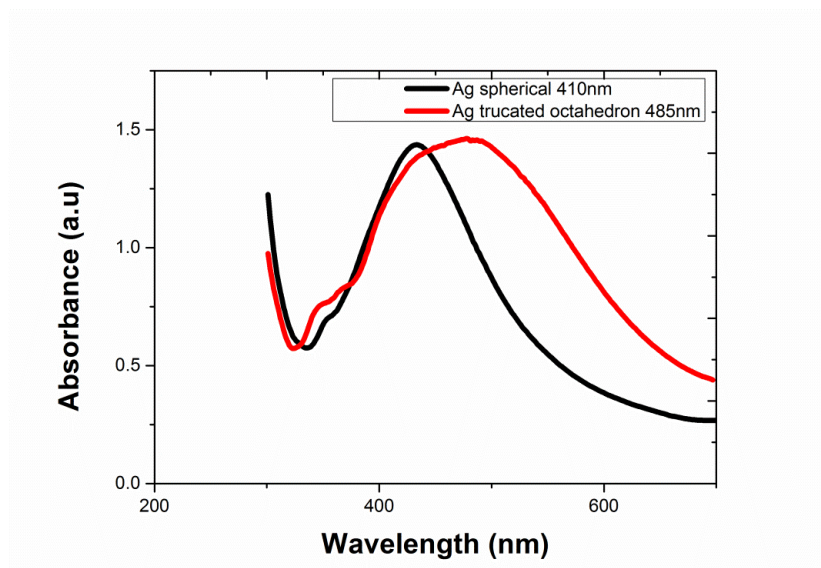


Figure 1: UV absorption spectra (a) AgNOct, (b) AgNS.

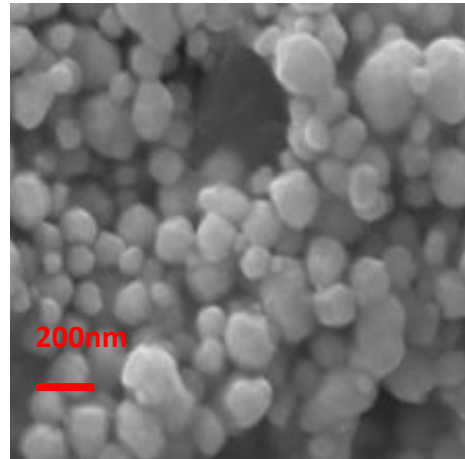
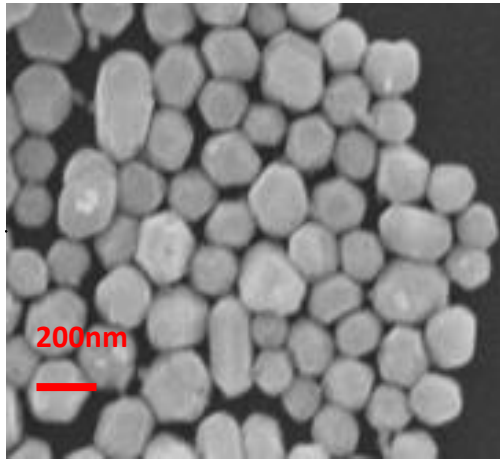


Figure 2: SEM images of (a) AgNOct, (b) AgNS.

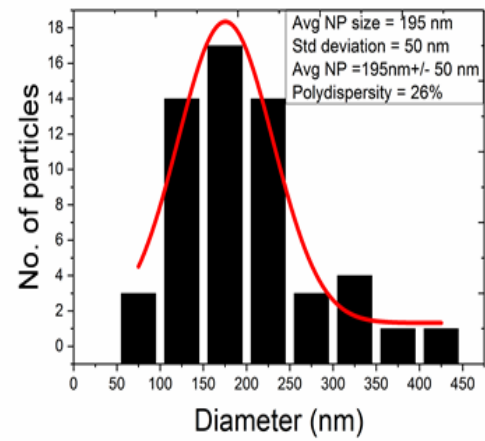
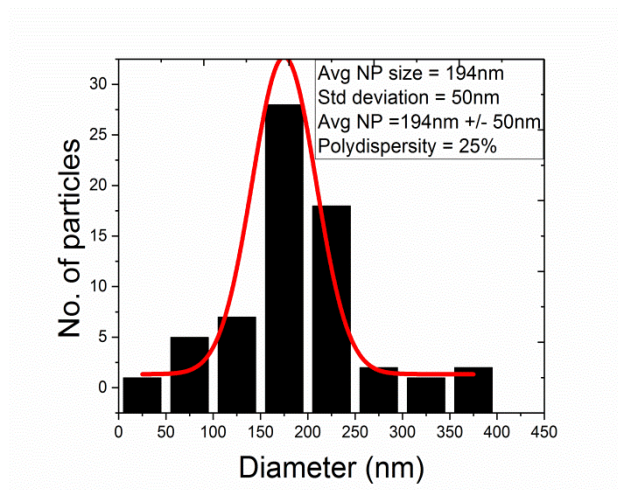


Figure 3: Size distribution for (a) AgNOct, (b) AgNS.

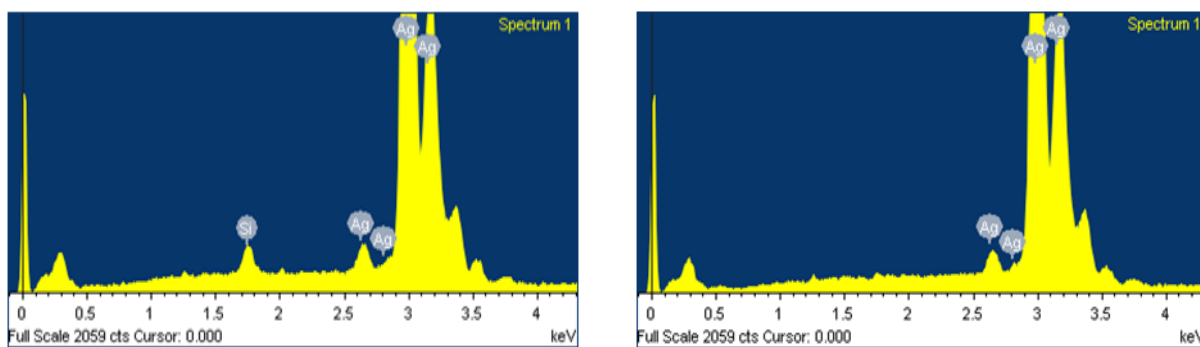


Figure 4: EDX of (a), AgNOct, (b) AgNS.

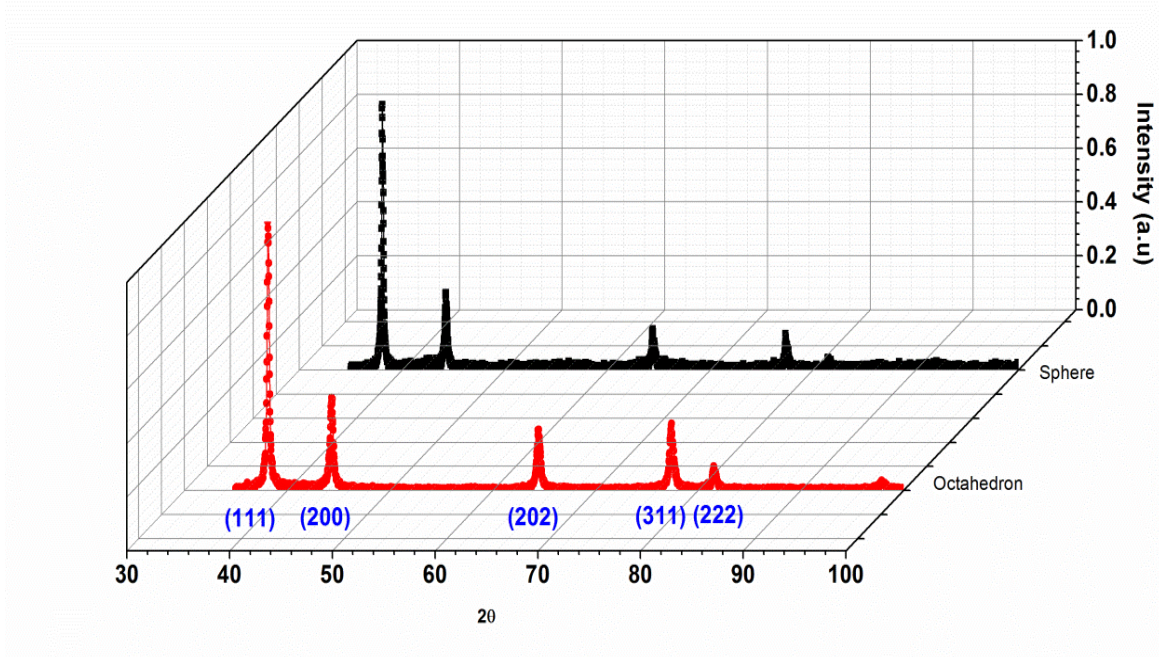


Figure 5: XRD pattern obtained from (a) AgNOct, (b) AgNS.

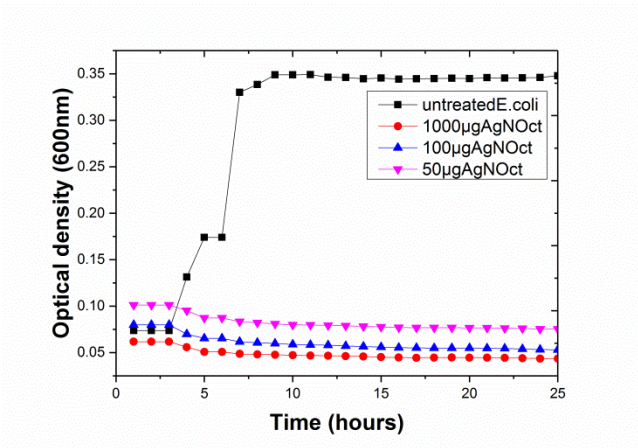


Figure 6: Growth curves (optical density) of *E. coli* treated with different concentration ($\mu\text{g/ml}$) of AgNO_3

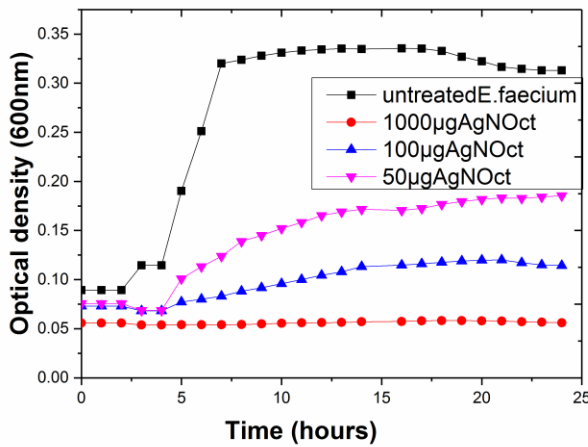


Figure 7: Growth curves (optical density) of *E. faecium* treated with different concentration ($\mu\text{g/ml}$) of AgNO_3 .

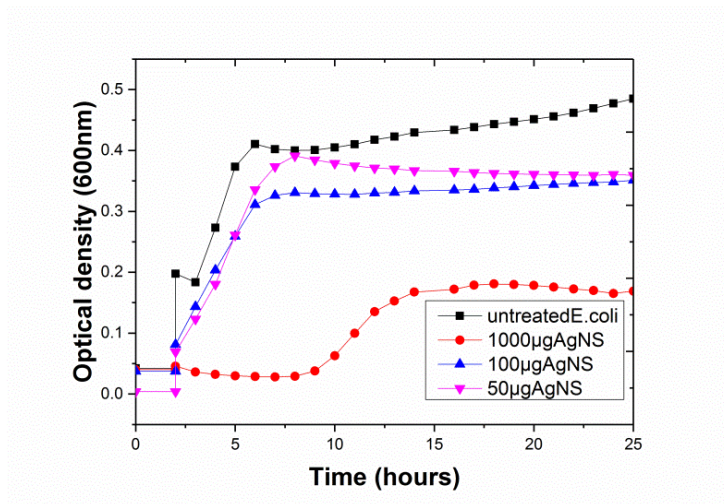


Figure 8: Growth curves (optical density) of *E. coli* treated with different concentration ($\mu\text{g/ml}$) of AgNS.

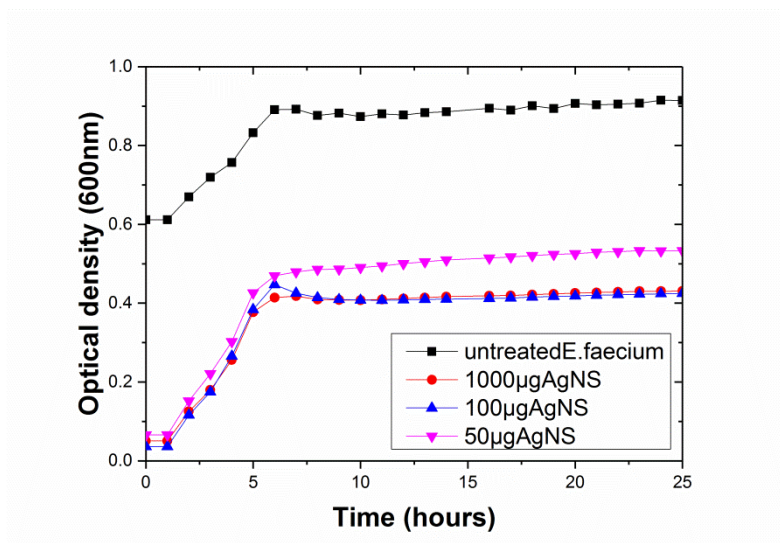


Figure 9: Growth curves (optical density) of *E. faecium* treated with different concentration ($\mu\text{g/ml}$) of AgNS.

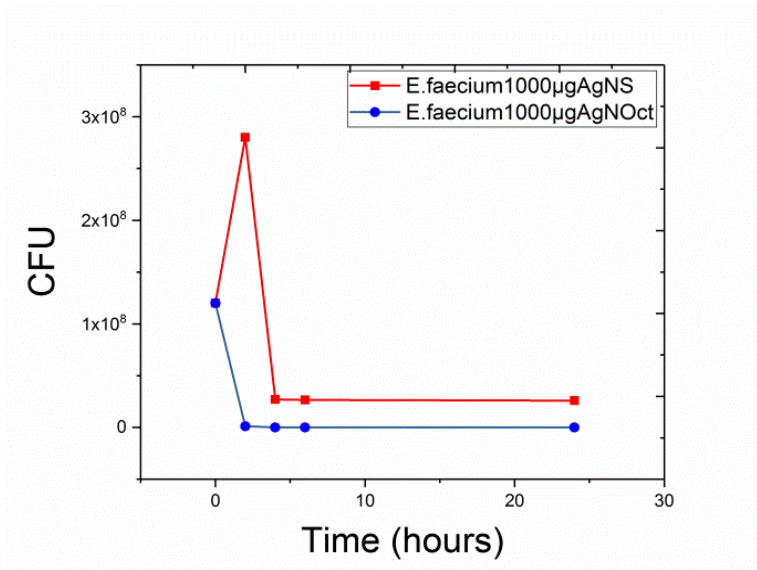


Figure 10: Viable count growth curves in the presence of AgNOct and AgNS for E.faecium.

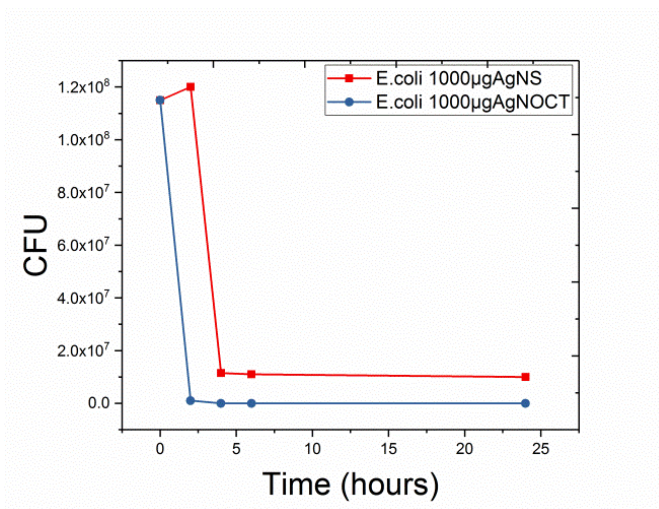


Figure 11: Viable count growth curves in the presence of AgNS and AgNOct for E.coli

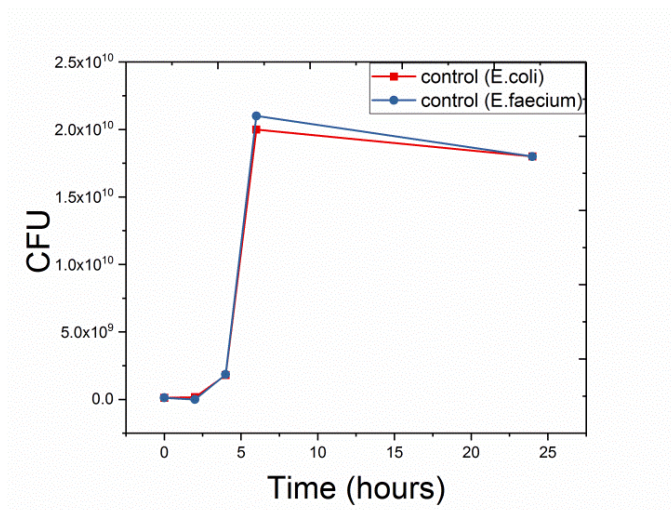


Figure 12: Viable count growth curves of untreated E.coli and E. faecium.

Time	Control E.coli	Control E.faecium	E.coli treated with AgNS	E.coli treated with AgNOct	Enterococcus treated with AgNS	Enterococcus treated with AgNoct
0 hours	115×10 ⁶	120×10 ⁶	115 × 10 ⁶ ±21	115 × 10 ⁶ ±21	120 × 10 ⁶ ±20	120 × 10 ⁶ ±20
2 hours	160×10 ⁶	165×10 ⁶	120 × 10 ⁶ ±21	100 × 10 ⁴ ±11	130 × 10 ⁶ ±11	115 × 10 ⁴ ± 23
4 hours	180×10 ⁷	185×10 ⁷	115 × 10 ⁵ ±17	No growth	125×10 ⁵ ±19	No growth
6 hours	200×10 ⁸	210×10 ⁸	110 × 10 ⁵ ±14	No growth	125 × 10 ⁵ ±15	No growth
24 hours	180×10 ⁸	180×10 ⁸	100 × 10 ⁵ ±24	No growth	120×10 ⁵ ±12	No growth

Table1 : Viable count growth curves in the presence of AgNOct and AgNS for *E.coli* and *E.faecium*

Shape-dependent antibacterial activity of silver nanoparticles on *Escherichia coli* and *Enterococcus faecium* bacterium

A, Alshareef¹, K, Laird² and R. B. M. Cross¹

¹Emerging Technologies Research Centre, School of Engineering and Sustainable Development, Faculty of Technology, De Montfort University, Leicester, LE19BH, United Kingdom; ²Leicester School of Pharmacy, Infectious Disease Research Group, Faculty of Health and Life Sciences, De Montfort University, Leicester, LE19BH, United Kingdom

Corresponding author: R. B. M. Cross, rcross@dmu.ac.uk, +00441162506157

Abstract: Silver nanoparticles (AgNPs) have been shown to exhibit strong antibacterial activity against both Gram-positive bacteria and Gram-negative bacteria including antibiotic resistant strains. This study aims to compare the bactericidal effect of different shaped AgNPs (spherical and truncated octahedral) against *Escherichia coli* and *Enterococcus faecium*. The antimicrobial activity of a range of concentrations (50, 100, 1000µg/ml) was determined over 24 hours using both optical density and viable counts. Truncated octahedral AgNPs (AgNOct) were found to be more active when compared with spherical AgNPs (AgNS). The difference in shape resulted in differences in efficacy which may be due to the higher surface area of AgNOct compared to AgNS, and differences in active facets and surface energies, with AgNPs having a bacteriostatic effect and AgNOct being bactericidal after 4 hours. The results suggest that AgNPs can be used as effective growth inhibitors in different microorganisms, rendering them applicable to various medical devices and antimicrobial control systems.

Keywords: AgNPs, shape-dependent, antibacterial activity, *Escherichia coli* and *Enterococcus faecium*

1-Introduction

Increasing numbers of microbial organisms are becoming resistant to antibiotics demonstrating a need for new, effective antibacterial agents [1]. In this regard, nanoscale materials have emerged as potential candidates in this area due to their unique physical and chemical properties [2]. The antibacterial effects of silver (Ag) salt are well known, and have been utilised to control bacterial growth in various devices and applications; these include catheters, dentistry, burn wounds, coated medical devices and water filtration [3] [4]. Moreover, a potential benefit of the use of nanoscale Ag particles (AgNPs) against microorganisms, e.g. *Escherichia coli* and *Enterococcus faecium* [5], is that such organisms are unlikely to build up resistance against AgNPs due to their broad spectrum of activity, unlike the narrow-targets of conventional antibiotics [6]. This activity includes the ability to attach through electrostatic interaction to the cell membrane and penetrate inside the bacteria, where they interact with sulphur-containing proteins and phosphorus containing compounds such as DNA [7]. Also, they have been shown to act upon the respiratory chain and replication of the bacterial cells leading to cell death [8].

The antibacterial activity of AgNPs against *E.coli* and *Streptococcus mutans* has been investigated previously and found to be size dependent, demonstrating that AgNPs of 5nm exhibit higher antibacterial activity when compared to 15nm and 55nm particles in Gram-positive and Gram-negative bacteria [9]. The antimicrobial efficacy of NPs can also depend on their shape. *Pal et al.* (2007) showed truncated triangular AgNPs exhibit *E.coli* inhibition at 1 µg; however, in order for spherical NPs to inhibit *E.coli* 12.5 µg was required, with rod NPs needing a total of 50 to 100 µg of silver content [7]. In our previous work, copper nanocubes showed enhanced antibacterial activity on *E.coli* and *E.faecium* compared with copper nanospheres [10]. This study aims to determine shape dependence (spherical and truncated octahedral) on the antimicrobial efficacy of AgNP against *E.coli* and *E.faecium*.

2-Experiment

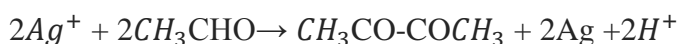
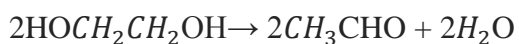
2.1-Materials

All chemicals for this work were purchased from Sigma-Aldrich, UK, without further purification. They include silver nitrate (AgNO_3), sodium bromide (NaBr),

polyvinylpyrrolidone (PVP) ($[C_6H_9NO]_n$), ethylene glycol (EG) ($C_2H_6O_2$) and sodium citrate ($C_6H_5Na_3$).

2.2-Synthesis of AgNOct

To synthesise AgNPOct, 3ml of two EG solutions, one containing 144mM PVP and 0.11mM NaBr, the other containing 94mM $AgNO_3$, were added dropwise via a two-channel syringe pump to 5ml of EG heated in a condenser at 160 °C. A 30 μ L drop of 10mM NaBr was then added to the pre-heated EG. The reaction solution turned yellow in a few seconds after the addition of $AgNO_3$ and PVP demonstrating the formation of AgNPs. After 10 minutes, the yellow colour faded in intensity due to oxidative etching and remained a light yellow colour for approximately 10 minutes before turning to brown and then to grey as the NPs increased in size. The synthesised NPs were then centrifuged at 4600rpm three times and washed with de-ionised water ((DI) 18.2M Ω MilliQ) to remove any impurities and unreacted precursors. The reactions governing the particles formation are expressed as follows [11]:

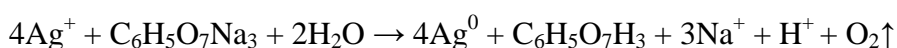


These reactions usually occur in the presence of a mediating species such as sodium bromide, sodium sulphide, sodium borohydride and hydrochloric acid. These mediators (NaBr in this case), play a role in the etching of the particle seeds, facilitating the formation of truncated octahedrons. The PVP also works as a shape-control agent prompting the reduction of $AgNO_3$ onto specific crystal faces while preventing reduction onto others.

2.3- Synthesis of AgNS

To synthesize spherical AgNPs, an aqueous solution of $AgNO_3$ 0.001M was heated to 100°C and then 3ml of sodium citrate was added. The mixture continued to be heated until the colour changed to yellow. To remove contamination and unreacted precursors from the AgNSs, a combination of centrifugation and DI water washes was used three times as before.

The particles were produced by reducing $AgNO_3$ through the following reaction [12]:



2.4-Particle characterisation

The AgNPs of both shapes were characterised using ultraviolet/visible (UV-VIS) spectroscopy (Evolution 300 UV-VIS, over the wavelength range 300nm to 700nm), scanning electron microscopy (SEM) and energy-dispersive X-ray (EDX) spectroscopy (LEO S430), and X-ray diffraction (XRD) Bruker D8 Advance diffractometer). The various solutions were drop-cast onto silicon and glass substrates for SEM/EDX and UV-VIS/XDR investigations respectively.

2.5-Antibacterial activity studies

All investigation were carried out in triplicate on at least two separate occasions

2.5.1-Bacterial strains and culture conditions

The antibacterial activities of the AgNPs were investigated using *E.coli* (NCTC8196) and *E.faecium* (NCTC12202) as models for Gram-negative bacteria and Gram-positive bacteria respectively. Bacteria strains were stored in Luria Bertani broth at -80°C; bacteria were then cultured in nutrient broth (NB) at 37 °C for 24 hours.

2.5.2- Screening of AgNPs for antibacterial activity

A disc diffusion method was used to determine the antibacterial activity of both shapes of AgNPs. In brief, overnight cultures of *E.coli* and *E. faecium* were spread-plated on to nutrient agar (NA), a 2cm paper disc was then impregnated with 50µl of 100µg/ml of both shapes of AgNPs and placed on the surface of the NA and incubated at 37°C for 24 hours. Zones of inhibition were then measured.

2.5.3-Determining the growth curve of *E. coli* and *E. faecium* bacteria cells exposed to different concentration of AgNPs using optical density

To investigate the growth kinetics curves of bacterial cells exposed to AgNPs different concentrations of both shapes (1000 µg, 100 µg and 50 µg) were used. Aliquots of 200µl of either *E.coli* or *E. faecium* in the presence of AgNPs were dispensed into 96-well plates. Optical densities (OD) were measured every hour (from 0 to 24 hour) at 600nm using a spectrophotometer (Spectra Max Plus 384). The control was wells containing bacteria only.

2.5.4-Viable count growth curves

An overnight culture of either *E. coli* or *E. faecium*, was inoculated into fresh NB (10^8) containing either AgNOct or AgNS of 1000 μ g/ml. The cultures were then incubated at 37 °C in a shaking incubator and samples taken at 0, 2, 4, 6 and 24 h. Aliquots of 100 μ l were spread-plated on to NA and incubated at 37 °C for 24h. Plates were then enumerated.

3-Results and discussion

The absorption spectrum of the AgNOct solution in Figure 1a shows an intense peak at 485nm with shoulders at 345nm and 365nm. The shape and position of plasmon absorption of AgNPs are mainly dependent on dielectric medium, particle size and the surface adsorbed species [5]. Anisotropic particles such as truncated octahedrons could have two or more SPR bands depending on the shape of the particles. However, only a single SPR band is present in the absorption spectra of spherical NPs. Figure 1b shows a sharp and intense peak at 410nm that is attributable to the surface plasmon absorption of spherical AgNPs [13].

SEM images of prepared AgNOct and AgNS are shown in Figure 2 (a and b respectively). The AgNOct have an average diameter of \sim 194nm. The size distribution is calculated from SEM images, where the polydispersity is 25% (Figure 3a). Figure 2b shows spherically-shaped NPs having an average diameter of \sim 195nm, where the polydispersity is 26% (Figure 3b). EDX analysis of the AgNPs shows the high purity of both sets of samples (Figure4 a and b).

XRD data shown in Figure 5 (a and b) confirms the formation of FCC AgNPs. Diffraction peaks at 2θ are 38, 44, 64, 77, 81, which are attributed to (111), (200), (202), (311) and (222) lattice planes of Ag with a cubic phase (JCPDS card no. 04-0783). AgNOct have higher intensities of (200), (202), (311) and (222) lattice planes compared with AgNS. Generally, spherical AgNPs exhibit a dominant (100) peak, while truncated octahedron AgNPs exhibit (111) with a lower intensity of (100). It has been reported previously that the reactivity of Ag is enhanced by high atomic density facets such as (111) [5][14]. It was postulated that atoms were more reactive on the facets of higher surface energy, which may

lead them to interact rapidly with oxygen-containing groups of lipopolysaccharide molecules that can result in enhanced attachment to the cell membrane [14].

Screening data shows that both shapes of AgNPs inhibit the growth of *E.coli* and *E. faecium* (the zone of inhibition was 2cm for both bacteria), as inhibition only occurred where there was direct contact with the AgNPs. The efficacy of spherical and truncated octahedral AgNPs was elucidated against *E.coli* and *E. faecium* using optical density. *E.coli* treated with AgNOct showed completely inhibited growth for all concentrations (1000, 100, 50 μ g) (Figure 6). However, there was limited growth in *E. faecium* at lower concentrations (50, 100 μ g), with only 1000 μ g completely inhibiting (Figure 7). Consequently the inhibitory effects were higher in *E.coli* compared with *E. faecium* for AgNOct.

Inhibition of *E.coli* treated with AgNS occurred at 10 hours with 1000 μ g/ml (Figure 8). For *E. faecium*, inhibition occurred in the first 6 hours at the same concentration and then limited growth began to occur (Figure 9). When viable count growth curves were generated in the presence of 1000 μ g/ml for both AgNOct and AgNS, the use of AgNOct against both bacteria resulted in the organisms being killed after 4 hours, demonstrating a bactericidal effect. Whereas, in the presence of AgNS there was only a modest reduction in CFU/mls in both organisms, demonstrating a bacteriostatic effect (Figure 10 and Figure 11). The viable count growth curves for untreated *E.coli* and *E. faecium* are shown in Figure 12 as a control.

The surface area of AgNOct was 1.32 m^2/g , while for AgNS it was 1.26 m^2/g . The data in Table 1 suggests that the shape effect on the antibacterial activity of AgNPs may be attributed to the higher surface areas and facet reactivity; AgNPs with larger effective contact areas and higher reactive facets exhibit stronger antibacterial activity [15]. Moreover, the antibacterial activity of AgNOct may be related to their geometric structure where AgNOct exhibit higher intensities than AgNSs of (200), (202), (311) and (222) lattice planes that might result in an increase in antibacterial activity.

The greater inhibitory effects observed in *E.coli* than in *E. faecium* are attributed to differences in the structure and thickness of the peptidoglycan layer of their cell walls. The peptidoglycan layer of Gram-positive bacteria such as *E. faecium* (~20-80nm) is thicker than that in Gram-negative bacteria such as *E. coli* (~7-8nm), as it includes linear polysaccharide chains cross-linked by short peptides to make a three dimensional rigid structure. This makes it more difficult for NPs to attach and penetrate [16]. In addition, the positively charged AgNPs are attracted electrostatically to the negatively charged

lipopolysaccharides and teichoic acids in Gram negative and Gram-positive bacteria respectively; this may lead to rupture and protein denaturation followed by cell death [17].

4-Conclusion

During this study AgNOct and AgNS were synthesised by a chemical reduction method in EG and DI water respectively. The NPs were characterised using UV-VIS, SEM, EDX and XRD. The antimicrobial efficacy of the AgNPs has been shown to be shape dependent against the organisms tested. AgNOct demonstrate bactericidal activity compared with bacteriostatic behaviour of AgNS. It is suggested that the bactericidal effect of AgNOct may be due to their geometric structure, higher surface area and higher surface energies when compared to AgNSs. This higher reactivity may ultimately lead to cell death more rapidly. Work is ongoing to determine more fully the mechanisms of action of the AgNPs that lead to the demonstrated bactericidal effects.

References

- [1] J. S. Kim, E. Kuk, K. N. Yu, J. Kim, S. J. Park, H. J. Lee, S. H. Kim, Y. K. Park, Y. H. Park and C. Hwang, "Antimicrobial effects of silver nanoparticles," *Nanomedicine: Nanotechnology, biology and medicine*, vol 3, no 1, pp. 95-101, 2007.
- [2] M. Rai, A. Yadav and A. Gade, "Silver nanoparticles as a new generation of antimicrobials," *Biotechnology advances*, vol 27, no 1, pp. 76-83, 2009.
- [3] M. Catauro, M. Raucci, F. De Gaetano and A. Marotta, "Antibacterial and bioactive silver-containing $\text{Na}_2\text{O} \cdot \text{CaO} \cdot 2\text{SiO}_2$ glass prepared by sol-gel method," *Journal of materials science: Materials in medicine*, vol 15, no 7, pp. 831-837, 2004.
- [4] J. H. Crabtree, R. J. Burchette, R. A. Siddiqi, I. T. Huen, L. L. Hadnott and A. Fishman, "The efficacy of silver-ion implanted catheters in reducing peritoneal dialysis-related infections," *Peritoneal dialysis international : Journal of the international society for peritoneal dialysis*, vol 23, no 4, pp. 368-374, Jul-Aug 2003.
- [5] S. Pal, Y. K. Tak and J. M. Song, "Does the antibacterial activity of silver nanoparticles depend on the shape of the nanoparticle? A study of the gram-negative bacterium escherichia coli," *Applied and environmental microbiology*, vol 73, no 6, pp. 1712-1720, Mar 2007.

- [6] G. Zhao and S. E. Stevens, "Multiple parameters for the comprehensive evaluation of the susceptibility of escherichia coli to the silver ion," *Biometals*, vol 11, no 1, pp. 27-32, 1998.
- [7] B. Sadeghi, F. S. Garmaroudi, M. Hashemi, H. Nezhad, A. Nasrollahi, S. Ardalan and S. Ardalan, "Comparison of the anti-bacterial activity on the nanosilver shapes: Nanoparticles, nanorods and nanoplates," *Advanced powder technology*, vol 23, no 1, pp. 22-26, 2012.
- [8] I. Sondi and B. Salopek-Sondi, "Silver nanoparticles as antimicrobial agent: A case study on E. coli as a model for gram-negative bacteria," *Journal of colloid and interface science*, vol 275, no 1, pp. 177-182, 2004.
- [9] Z. Lu, K. Rong, J. Li, H. Yang and R. Chen, "Size-dependent antibacterial activities of silver nanoparticles against oral anaerobic pathogenic bacteria," *Journal of materials science: Materials in medicine*, vol 24, no 6, pp. 1465-1471, 2013.
- [10] A. Alshareef, K. Laird and R. Cross, "Chemical synthesis of copper nanospheres and nanocubes and their antibacterial activity against escherichia coli and enterococcus sp." *Acta metallurgica sinica (english letters)*, pp. 1-7, 2016.
- [11] B. Gupta, W. Rouesnel and J. J. Gooding, "The role of oxygen in synthesizing monodisperse silver nanocubes," *Australian journal of chemistry*, vol 64, no 11, pp. 1488-1493, 2011.
- [12] C. RATYAKSHI. R.P, " Colloidal synthesis of silver nano particles " *Asian journal of chemistry*, vol Vol. 21, no No. 10, pp. S113-116, 2009.
- [13] M. Guzman, J. Dille and S. Godet, "Synthesis and antibacterial activity of silver nanoparticles against gram-positive and gram-negative bacteria," *Nanomedicine: Nanotechnology, biology and medicine*, vol 8, no 1, pp. 37-45, 2012.
- [14] Y. Xia, Y. Xiong, B. Lim and S. E. Skrabalak, "Shape Controlled synthesis of metal nanocrystals: Simple chemistry meets complex physics?" *Angewandte chemie international edition*, vol 48, no 1, pp. 60-103, 2009.
- [15] X. Hong, J. Wen, X. Xiong and Y. Hu, "Shape effect on the antibacterial activity of silver nanoparticles synthesized via a microwave-assisted method," *Environmental science and pollution research*, vol 23, no 5, pp. 4489-4497, 2016.
- [16] W. Wang, L. Geng, S. Ding and S. Xu, , "Facile synthesis of silver nanoparticles and their antimicrobial activity against several representative microbial species," In *Biomedical engineering and biotechnology (iCBEB), 2012 international conference on*, 2012, pp. 287-290.
- [17] A. M. Fayaz, K. Balaji, M. Girilal, R. Yadav, P. T. Kalaichelvan and R. Venketesan, "Biogenic synthesis of silver nanoparticles and their synergistic effect with antibiotics: A study against gram-positive and gram-negative bacteria," *Nanomedicine: Nanotechnology, biology and medicine*, vol 6, no 1, pp. 103-109, 2010.

List of Figures:

Figure 1: UV absorption spectra (a) AgNOct, (b) AgNS.

Figure 2: SEM images of (a) AgNOct, (b) AgNS.

Figure 3: Size distribution for (a) AgNOct, (b) AgNS.

Figure 4: EDX of (a), AgNOct, (b) AgNS.

Figure 5: XRD pattern obtained from (a) AgNOct, (b) AgNS.

Figure 6: Growth curves (optical density) of *E.coli* treated with different concentration ($\mu\text{g/ml}$) of AgNOct

Figure 7: Growth curves (optical density) of *E.faecium* treated with different concentration ($\mu\text{g/ml}$) of AgNOct.

Figure 8: Growth curves (optical density) of *E.coli* treated with different concentration ($\mu\text{g/ml}$) of AgNS.

Figure 9: Growth curves (optical density) of *E.faecium* treated with different concentration ($\mu\text{g/ml}$) of AgNS.

Figure 10: Viable count growth curves in the presence of AgNOct and AgNS for *E.faecium*.

Figure 11: Viable count growth curves in the presence of AgNS and AgNOct for *E.coli*

Figure 12: Viable count growth curves of untreated *E.coli* and *E. faecium*.

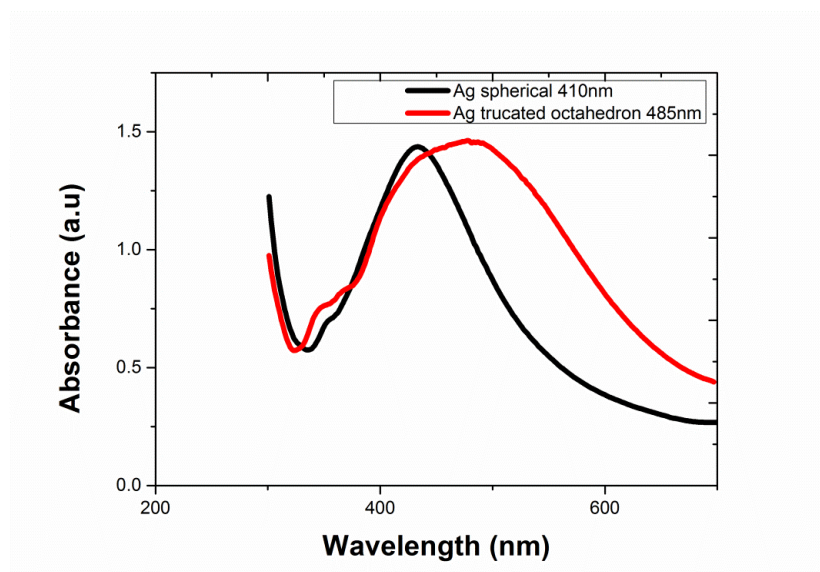


Figure 1: UV absorption spectra (a) AgNOct, (b) AgNS.

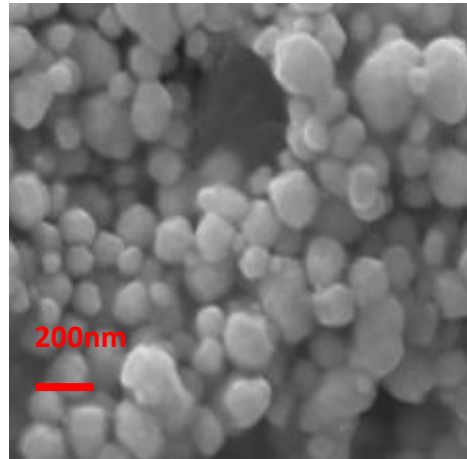
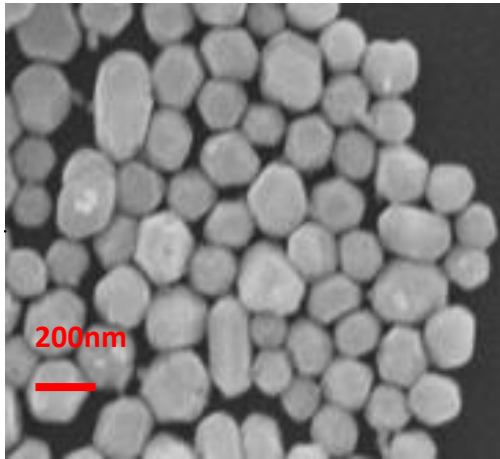


Figure 2: SEM images of (a) AgNOct, (b) AgNS.

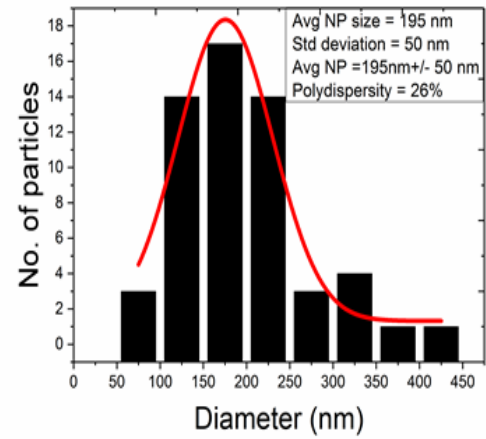
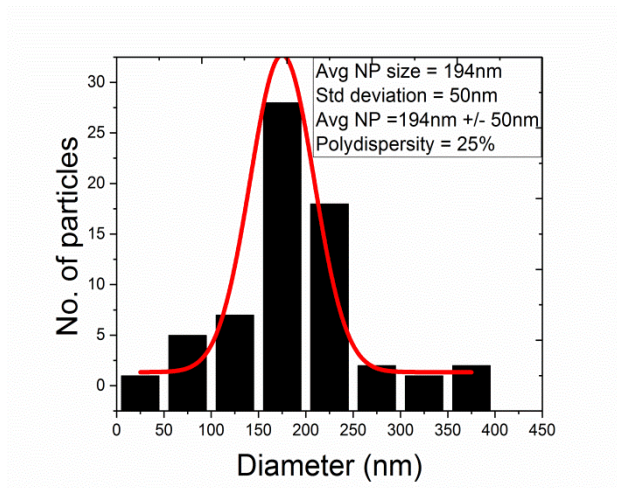


Figure 3: Size distribution for (a) AgNOct, (b) AgNS.

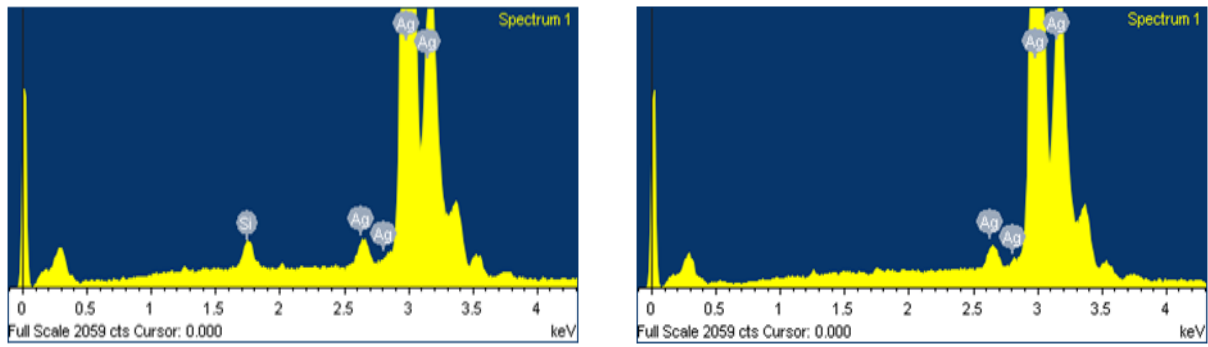


Figure 4: EDX of (a), AgNOct, (b) AgNS.

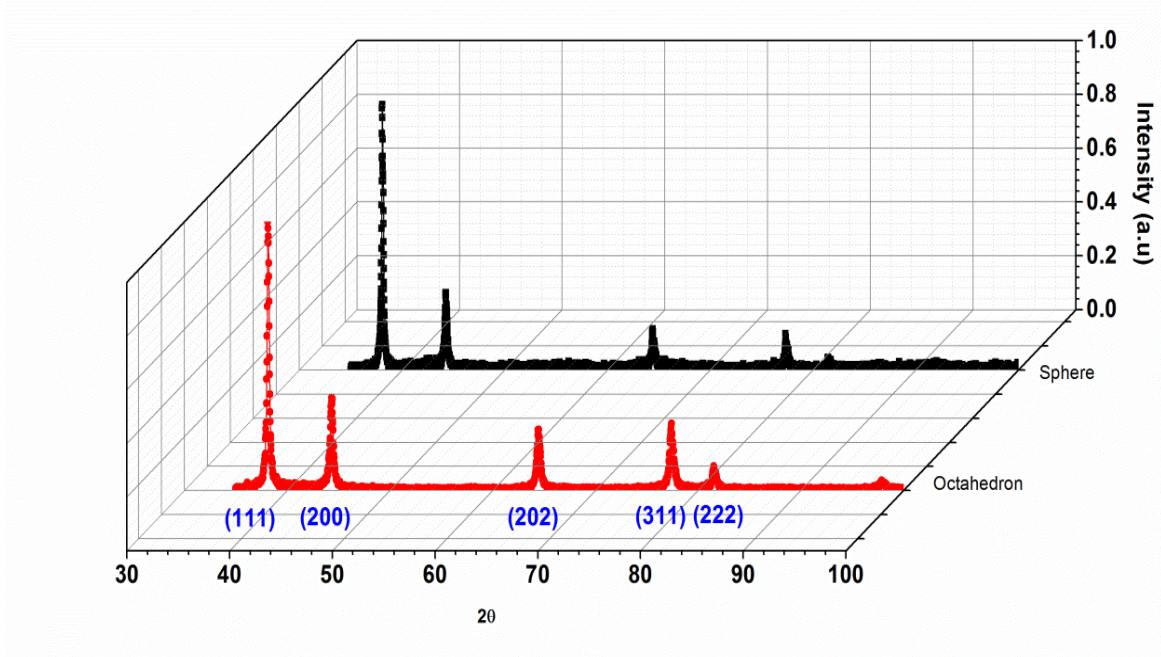


Figure 5: XRD pattern obtained from (a) AgNOct, (b) AgNS.

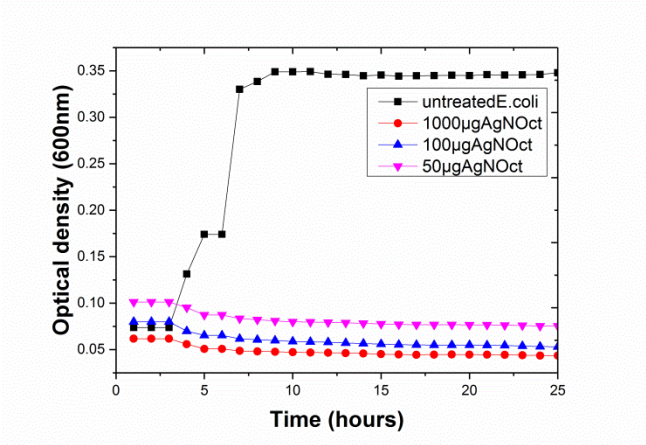


Figure 6: Growth curves (optical density) of *E. coli* treated with different concentration ($\mu\text{g/ml}$) of AgNO_3

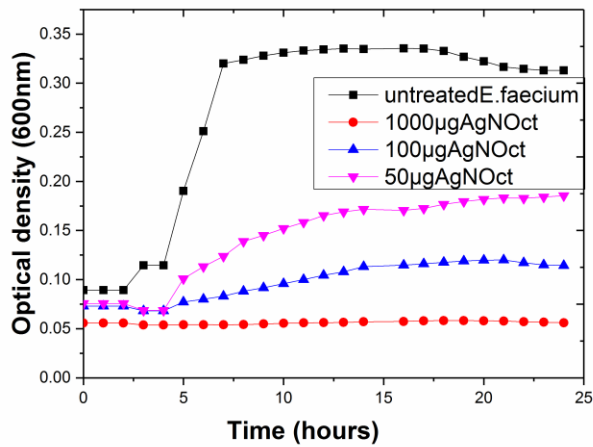


Figure 7: Growth curves (optical density) of *E. faecium* treated with different concentration ($\mu\text{g/ml}$) of AgNO_3 .

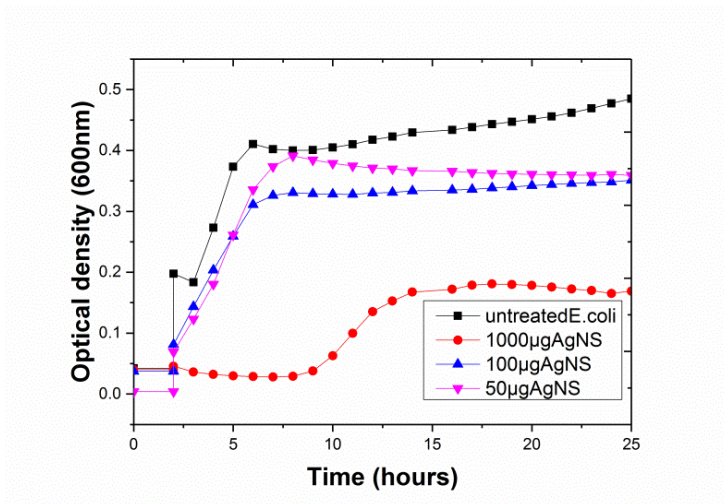


Figure 8: Growth curves (optical density) of *E. coli* treated with different concentration ($\mu\text{g/ml}$) of AgNS.

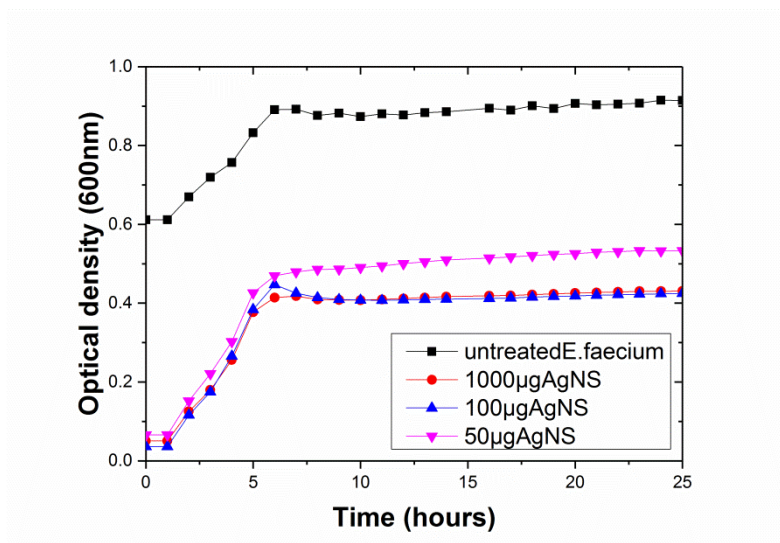


Figure 9: Growth curves (optical density) of *E. faecium* treated with different concentration ($\mu\text{g/ml}$) of AgNS.

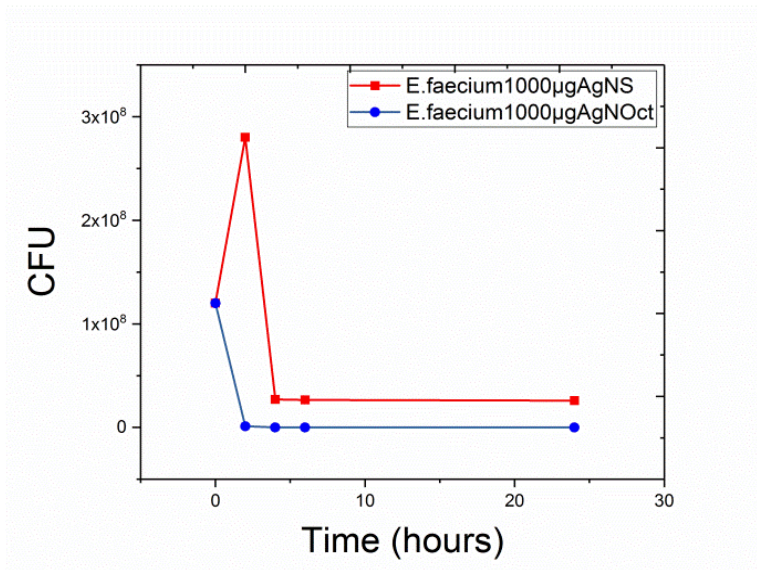


Figure 10: Viable count growth curves in the presence of AgNOct and AgNS for E.faecium.

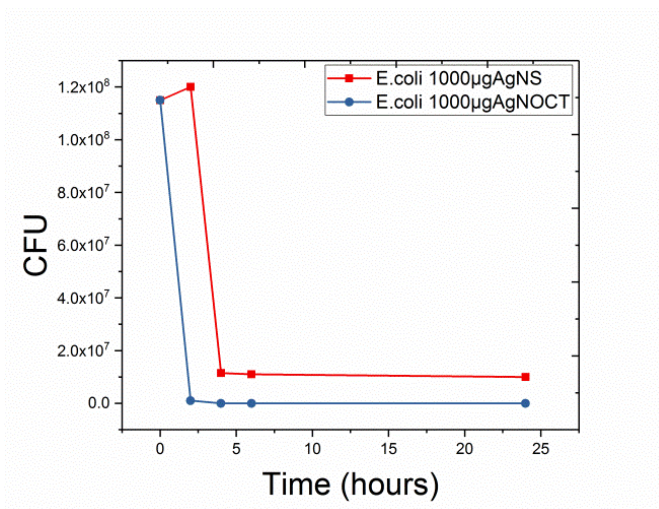


Figure 11: Viable count growth curves in the presence of AgNS and AgNOct for E.coli

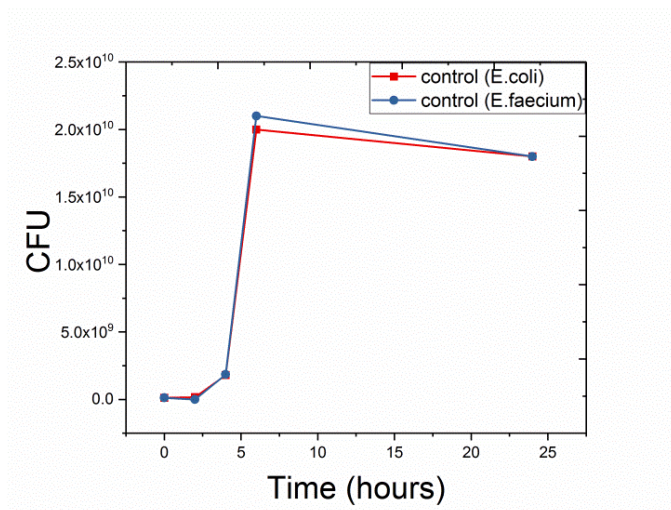


Figure 12: Viable count growth curves of untreated E.coli and E. faecium.

Time	Control E.coli	Control E.faecium	E.coli treated with AgNS	E.coli treated with AgNOct	Enterococcus treated with AgNS	Enterococcus treated with AgNoct
0 hours	115×10 ⁶	120×10 ⁶	115 × 10 ⁶ ±21	115 × 10 ⁶ ±21	120 × 10 ⁶ ±20	120 × 10 ⁶ ±20
2 hours	160×10 ⁶	165×10 ⁶	120 × 10 ⁶ ±21	100 × 10 ⁴ ±11	130 × 10 ⁶ ±11	115 × 10 ⁴ ± 23
4 hours	180×10 ⁷	185×10 ⁷	115 × 10 ⁵ ±17	No growth	125×10 ⁵ ±19	No growth
6 hours	200×10 ⁸	210×10 ⁸	110 × 10 ⁵ ±14	No growth	125 × 10 ⁵ ±15	No growth
24 hours	180×10 ⁸	180×10 ⁸	100 × 10 ⁵ ±24	No growth	120×10 ⁵ ±12	No growth

Table1 : Viable count growth curves in the presence of AgNOct and AgNS for *E.coli* and *E.faecium*

Time	Control E.coli	Control E.faecium	E.coli treated with AgNS	E.coli treated with AgNOct	Enterococcus treated with AgNS	Enterococcus treated with AgNoct
0 hours	115×10^6	120×10^6	115×10^6 ± 21	115×10^6 ± 21	$120 \times 10^6 \pm 20$	$120 \times 10^6 \pm 20$
2 hours	160×10^6	165×10^6	120×10^6 ± 21	100×10^4 ± 11	$130 \times 10^6 \pm 11$	$115 \times 10^4 \pm 23$
4 hours	180×10^7	185×10^7	115×10^5 ± 17	No growth	$125 \times 10^5 \pm 19$	No growth
6 hours	200×10^8	210×10^8	110×10^5 ± 14	No growth	$125 \times 10^5 \pm 15$	No growth
24 hours	180×10^8	180×10^8	100×10^5 ± 24	No growth	$120 \times 10^5 \pm 12$	No growth

Table1 : Viable count growth curves in the presence of AgNOct and AgNS for *E.coli* and *E.faecium*

Figure

[Click here to download Figure: ICPAM figures Alanod Alshareef.docx](#)

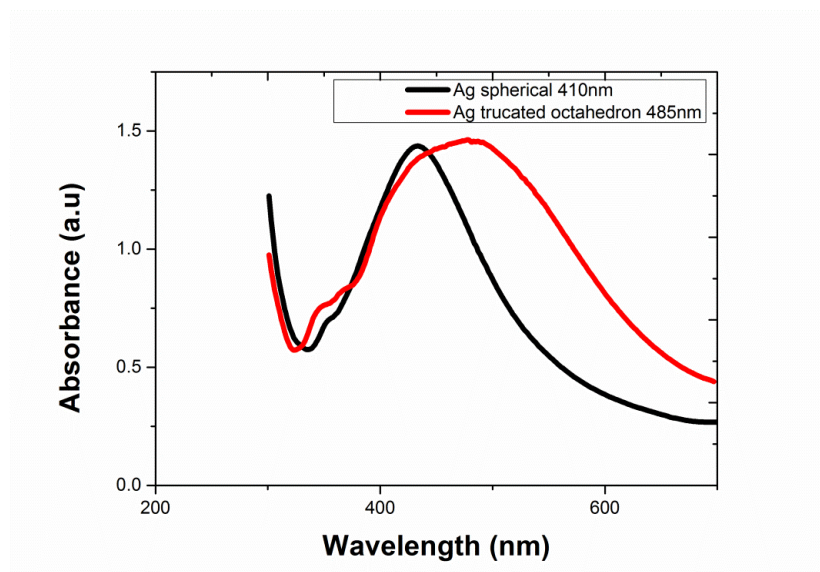


Figure 1: UV absorption spectra (a) AgNOct, (b) AgNS.

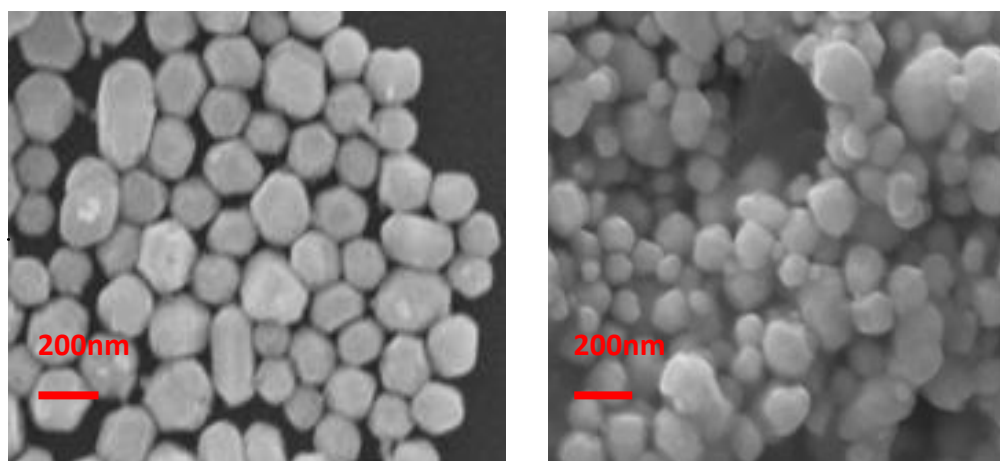


Figure 2: SEM images of (a) AgNOct, (b) AgNS.

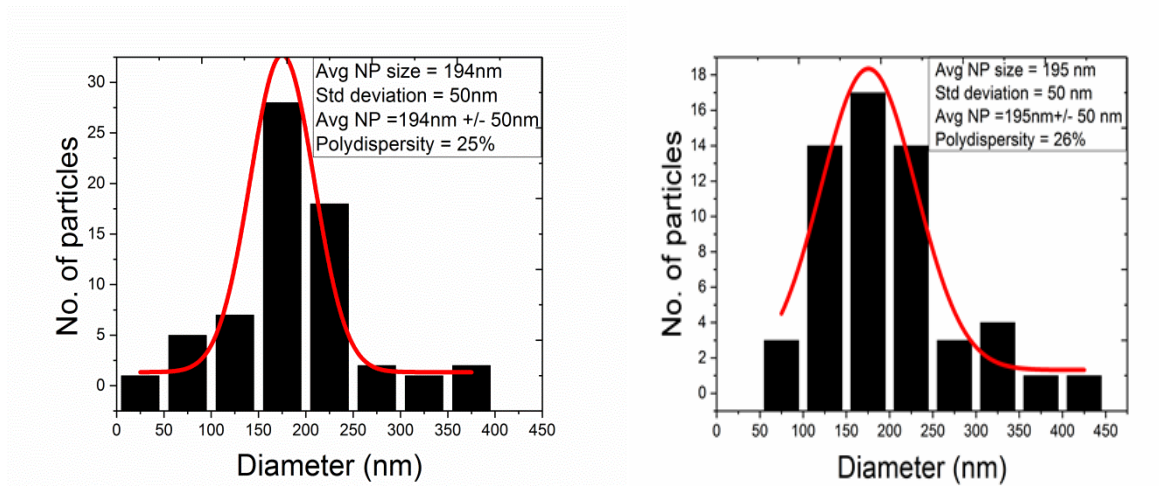


Figure 3: Size distribution for (a) AgNOct, (b) AgNS.

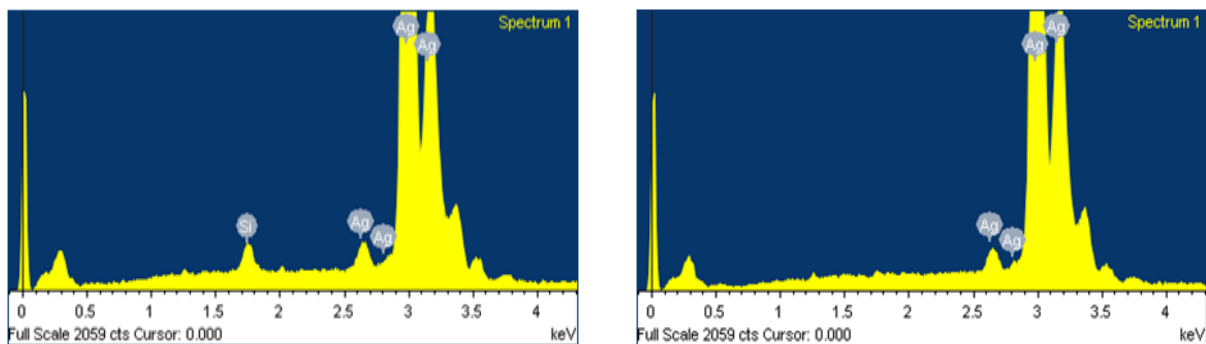


Figure 4: EDX of (a), AgNOct, (b) AgNS.

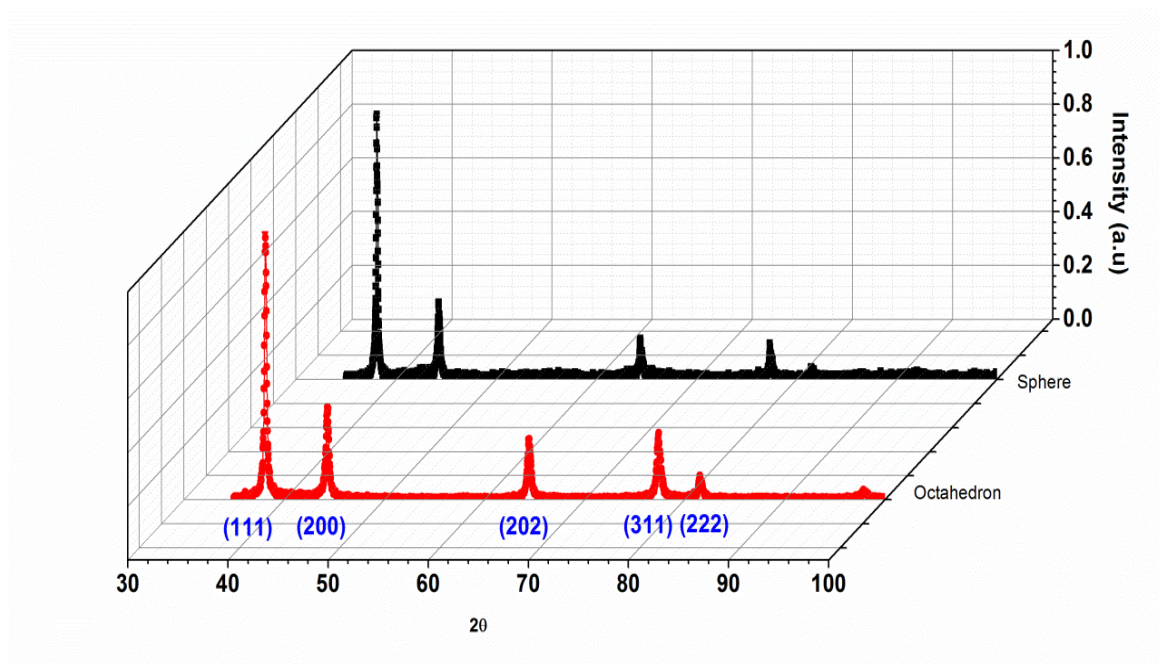


Figure 5: XRD pattern obtained from (a) AgNOct, (b) AgNS.

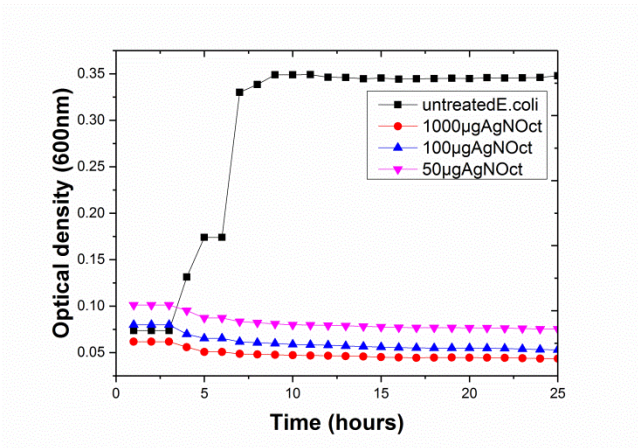


Figure 6: Growth curves (optical density) of E.coli treated with different concentration ($\mu\text{g/ml}$) of AgNO₃

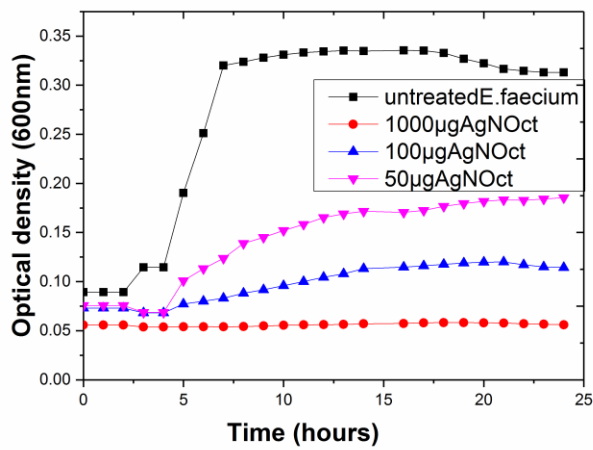


Figure 7: Growth curves (optical density) of E.faecium treated with different concentration ($\mu\text{g/ml}$) of AgNO₃.

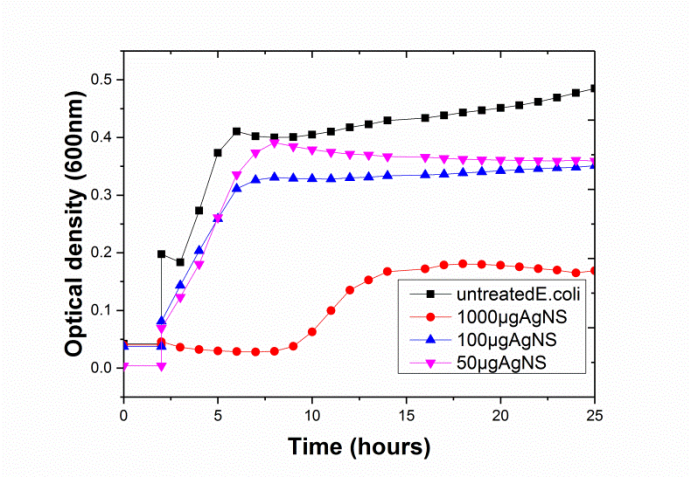


Figure 8: Growth curves (optical density) of *E.coli* treated with different concentration ($\mu\text{g/ml}$) of AgNS.

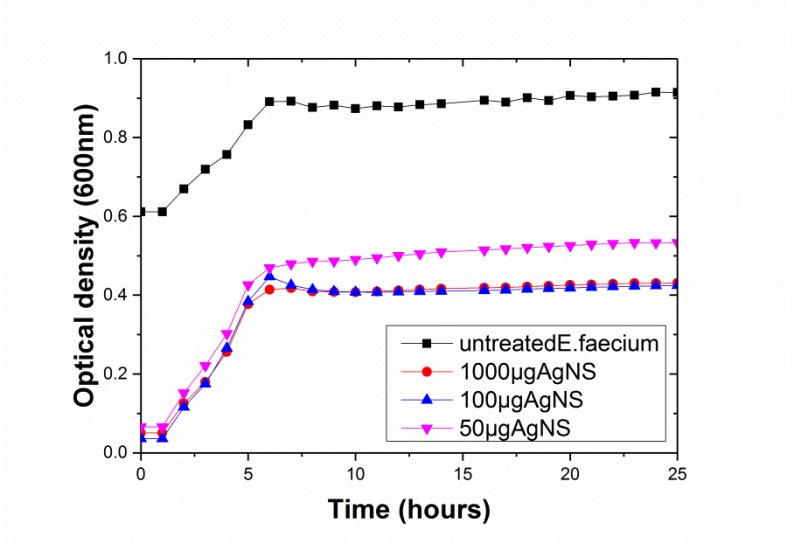


Figure 9: Growth curves (optical density) of *E.faecium* treated with different concentration ($\mu\text{g/ml}$) of AgNS.

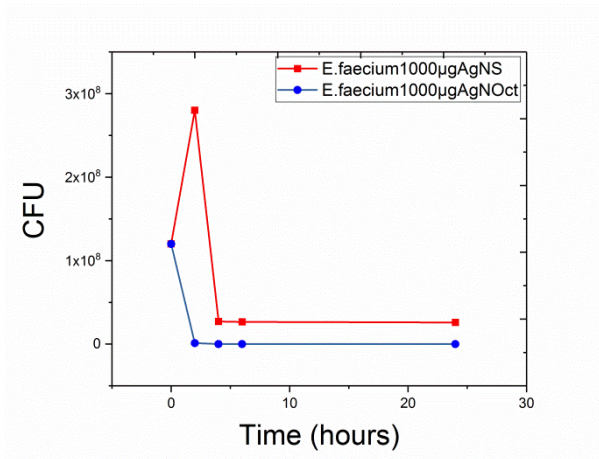


Figure 10: Viable count growth curves in the presence of AgNOct and AgNS for *E. faecium*.

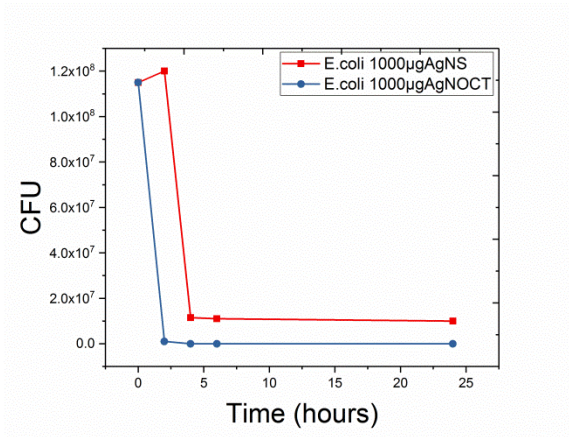


Figure 11: Viable count growth curves in the presence of AgNOct and AgNS for *E. coli*

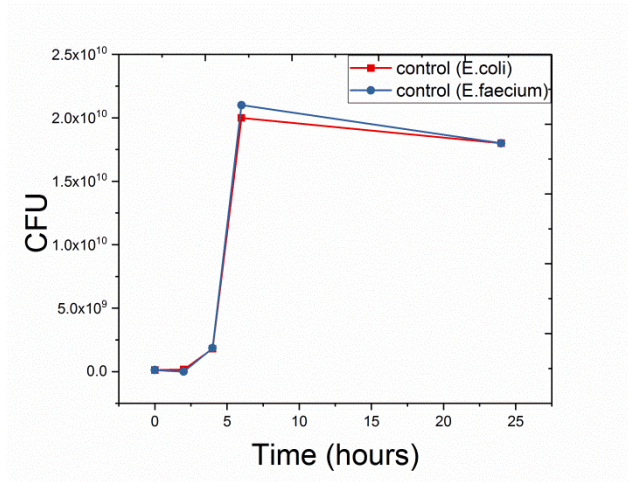


Figure 12: Viable count growth curves of untreated *E. coli* and *E. faecium*.